Water Research 182 (2020) 116012

Contents lists available at ScienceDirect

Water Research

journal homepage: www.elsevier.com/locate/watres

Anionic nanoparticle and microplastic non-exponential distributions from source scale with grain size in environmental granular media

William P. Johnson [a, *], Anna Rasmuson [a], Cesar Ron [a], Brock Erickson [a], Kurt VanNess [a], Diogo Bolster [b], Brett Peters [b]

[a] Dept. of Geology and Geophysics, University of Utah, Salt Lake City, UT, 84112, USA
[b] Dept. of Civil and Environmental Engineering and Earth Sciences, University of Notre Dame, Notre Dame, IN, 46556, USA

ARTICLE INFO

Article history:
Received 5 March 2020
Received in revised form
27 May 2020
Accepted 1 June 2020
Available online 6 June 2020

Keywords:
Nanoparticles
Microplastics
Colloids
Groundwater
Transport
Retention

ABSTRACT

Nanoparticle and microplastic (colloid) transport behaviors impact strategies for groundwater protection and remediation. Complex colloid transport behaviors of anionic nano- and micro-sized colloids have been previously elucidated *via* independent experiments in chemically-cleaned and amended granular media with grain sizes in the range of fine to coarse sand (e.g., 200–1000 μm). Such experiments show that under conditions where a repulsive barrier was present in colloid-collector interactions (unfavorable conditions), the distribution of retained colloids down-gradient from their source deviates from the exponential decrease expected from compounded loss across a series of collectors (grains). Previous experiments have not examined the impact of colloid size or granular media grain size on colloid distribution down-gradient from their source, particularly in streambed-equilibrated granular media. To address this gap, a field transport experiment in constructed wetland stream beds to distances up to 20 m were conducted for colloids ranging in size from micro to nano (60 nm–7 μm) in streambed-equilibrated pea gravel and sand (4200 and 420 μm mean grain sizes, respectively). All colloid sizes showed non-exponential (hyper-exponential) distributions from source, over meter scales in pea gravel versus cm scales reported for fine sand. Colloids in the *ca.* 1 μm size range were most mobile, as expected from mass transfer to surfaces and interaction with nanoscale heterogeneity. The distance over which non-exponential colloid distribution occurred increased with media grain size, which carries implications for the potential mechanism driving non-exponential colloid distribution from source, and for strategies to predict transport.

1. Introduction

An ability to predict transport behaviors of suspended nano-to micro-scale particles (herein referred to as colloids) in environmental granular media is needed to support groundwater resource protection, including prediction of pathogen transport distances (e.g., Borchardt et al., 2003; Worthington and Smart, 2017; Ray et al., 2019) and contaminant remediation *via* delivery of novel nano- and micro-particles (e.g., Zhang et al., 2003; Scheibe et al., 2011; Laumann et al., 2014). Anionic (e.g., carboxylate-modified) commercial nano- and micro-beads are used as surrogates for pathogens and other microbes in transport studies; however, they are more recently used as representatives of nanoparticle and microplastic contaminants (e.g., Zhang et al., 2003; Panno et al., 2019; Zhang et al., 2020) because of the near-neutral density of microplastics, as well as the fact that commercial plastic microbeads are an emerging concern in their own right due to their presence in personal care products that are a major component of microplastic flux in terrestrial aquatic systems (e.g., Anderson et al., 2016).

Current understanding of colloid transport behavior largely comes from highly controlled laboratory experiments in cleaned uniform granular media of fine to coarse sand grain size (e.g., Li et al., 2004; Tufenkji and Elimelech, 2004; Tong et al., 2005; Tong and Johnson, 2006; Wang et al., 2014). These experiments demonstrate that when a repulsive barrier to attachment is absent (favorable conditions for attachment) the distribution of retained colloids down-gradient from their source is exponential, as expected from their compounded loss for each grain passed in series (e.g., Li et al.,

* Corresponding author.
E-mail address: william.johnson@utah.edu (W.P. Johnson).

https://doi.org/10.1016/j.watres.2020.116012
0043-1354/

2004; Johnson and Hilpert, 2013). In contrast, the distribution from source deviates from exponential when a repulsive barrier to attachment is present (unfavorable conditions); that is, faster than exponential (hyper-exponential), or alternatively with a maximum retained concentration down-gradient from the source (non-monotonic) (e.g., Albinger et al., 1994; Harvey et al., 1995; Bolster et al., 1999; Schijven et al., 1999; Bradford et al., 2002; Li et al., 2004; Tufenkji and Elimelech, 2004a; Tufenkji et al., 2004; Li and Johnson, 2005; Tong and Johnson, 2007; Liang et al., 2013; Wang et al., 2014).

However, the relevance of the above-described transport behaviors to groundwater and hyporheic granular media remains unclear for several reasons. Colloids of environmental concern typically have negative ζ−potentials in groundwater (anionic), including biological colloids (e.g., viruses, bacteria and protozoa) (e.g., Ryan et al., 1999; Foppen and Schijven, 2006; Liu et al., 2009). Existing transport experiments elucidating the above-described behaviors have primarily utilized chemically-cleaned and uniform granular silicate mineral media (e.g. silica and quartz) to ensure dominance of their intrinsic charge that is negative across the pH range typical of groundwater (e.g., 7−9) (e.g., Li et al., 2004; Tufenkji and Elimelech, 2004a; Tufenkji et al., 2004; ; Tufenkji and Elimelech, 2005a,b; Tong and Johnson, 2007; Liang et al., 2013; Wang et al., 2014). Less sorted and non-cleaned granular media may include clay minerals with intrinsically contrasting negative (faces) versus positive (edges) surfaces (e.g., Schwarzenbach et al., 1993), and potential patches of oxyhydroxides of iron, aluminum, and manganese that may carry positive or neutral surface charge at groundwater pH (e.g., Schwarzenbach et al., 1993; Laumann et al., 2013; Trauscht et al., 2015). Because intrinsic surface characteristics are moderated by nanoscale surface roughness (Bhattacharjee, 1998; Bendersky and Davis, 2011; Jin et al., 2015; Rasmuson et al., 2017; Rasmuson et al., 2019a), sorption of natural organic matter (Tipping and Cooke, 1982; Davis, 1982; Jardine et al., 1989; Johnson et al., 1996; Johnson and Logan, 1996; Foppen et al., 2008; Wang et al., 2012; Han et al., 2014; Scholl and Harvey, 1992; Franchi & O'Melia, 2003; Liu et al., 2007; Pelley and Tufenkji, 2008), and major ion concentrations (Israelachvili, 2011; Huynh and Chen, 2011; Akaighe et al., 2012; Baalousha et al., 2013), the impact of these on non-exponential colloid distribution needs also to be determined. To address this need, some laboratory transport experiments examined chemically-cleaned sediment subsequently equilibrated with specific components of organic matter (e.g., Suwannee River humic acid) (Johnson and Logan, 1996) and natural field sediment (Bolster et al., 1999; Gupta et al., 2009; Rasmuson et al., 2019b). Limited field studies indicate non-exponential colloid distribution from source (Schijven et al., 1999; 2000; Johnson et al., 2001; Zhang et al., 2001) based on greater apparent colloid retention rate coefficients at near (e.g., few meters) versus greater distances from source. However, this conclusion is weakened by fluid velocity variations with distance from source that result from the intersecting radial flow fields imposed by coupled injection and extraction. Furthermore, injected microbes used in many laboratory, and all reported field, studies are potentially impacted by physiological (e.g., death or inactivation) (John and Rose, 2005) and ecological processes (e.g., predation) acting on injected bacteria or viruses (Levin et al., 1977; Lenski, 1988; Schivjen et al., 2000; Zhang et al., 2001).

Despite the above limitations, existing studies suggest that non-exponential colloid distribution from source occurs in natural granular media, and therefore presents challenges for transport prediction related to groundwater protection and remediation. However, understanding the mechanism underlying observed non-exponential colloid distribution from source requires assessing the impact of colloid size and granular media grain size on non-exponential distribution, which was not performed in previous experiments. The purpose of this study was therefore to examine colloid distributions from source in streambed-equilibrated granular media ranging in mean grain size from fine sand to pea gravel for colloid sizes ranging from nano-to micro-scale. Because many reports already exist for non-exponential colloid distribution in sand-sized granular media, the focus here was on coarser media, although sand was included to demonstrate that transport distances were consistent with previous reports, and that the impact of colloid size was consistent with coarser media.

2. Materials and methods

2.1. Site and granular media description

Colloid transport experiments were performed in October 2018 in constructed stream/wetland channels at the Notre Dame Linked Experimental Ecosystem Facility (ND-LEEF) (Fig. 1) in St Joseph County, Indiana. Channel shapes were trapezoidal in cross section, with dimensions 12.7 cm depth × 12.7 cm basal width × 40.6 cm surface width, and with channel lengths of 19.5 m and 4.9 m for pea gravel and sand granular media (described below), respectively (Fig. 1). Channels were lined with impermeable concrete at the base and sides to ensure constant discharge and fluid velocity with transport distance (Fig. 1). Channel elevation gradient was 0.0075 for both channels. The channels are hydrologically isolated from surrounding flow via a rubber liner, and surface flow is minimal due to porous site soils and vegetation that extends to the channel margin (Supplementary Material, Figs. S1 and S2).

Pea gravel and sand were the granular media used in the two channels (Supplementary Material, Fig. S2). Pea gravel was obtained from a local pit excavator (St Joseph River floodplain, South Bend, IN) and provider of alluvial materials (not crushed). Sand was obtained from a local concrete factory (Hanson-Heidelberg Cement Group, Thornton IL). Grain size distributions measured *via* sieving 200 g of material produced mode and mean diameters of approximately 4.3 and 4.2 mm, respectively for pea gravel (both wet and dry sieved), and approximately 0.05 and 0.42 mm, respectively for sand (Supplementary Material, Fig. S3). Gravimetrically determined porosities were approximately 0.35 and 0.25 for the pea gravel and sand, respectively, consistent with the relatively uniformity of grain size for the pea gravel. Granular media were equilibrated under ambient streambed conditions for six months (April through September) prior to the transport experiment (Supplementary Material, Fig. S1). At the end of the growing season (October 2018), algae stringers were visible at the granular media surface (Supplementary Material, Fig. S1), and visible organic matter was suspended from the subsurface granular media during excavation and extraction from both granular media at the end of the experiment. Because sediment surface chemistries were purposefully altered by natural organic matter during streambed equilibration, mineralogical analyses were not performed. The alluvial origin of the sediments suggests dominance of silicate mineralogy (quartz, silica, feldspars), which display negative ζ-potentials at the pH of the transport experiment (Trauscht et al., 2015).

Channel source water had a pH of 8.1, conductance of 550 μS/cm, ionic strength (IS) of 20 mM, dominated by Ca^{2+}, Mg^{2+}, SO_4^{2-}, and carbonate species, and a dissolved organic carbon content of ~11.5 mg/L. Flow in the constructed channels was sourced *via* pump from a nearby reservoir that was supplied by local groundwater. During the six months preceding the colloid transport experiment, flow to the channels was sufficient (approximately 48 L/min) to maintain approximately 3.5 cm water column depth above the sediment surface. Seven days prior to and during the colloid transport experiment, flow was reduced to 200 ml/min (pea gravel)

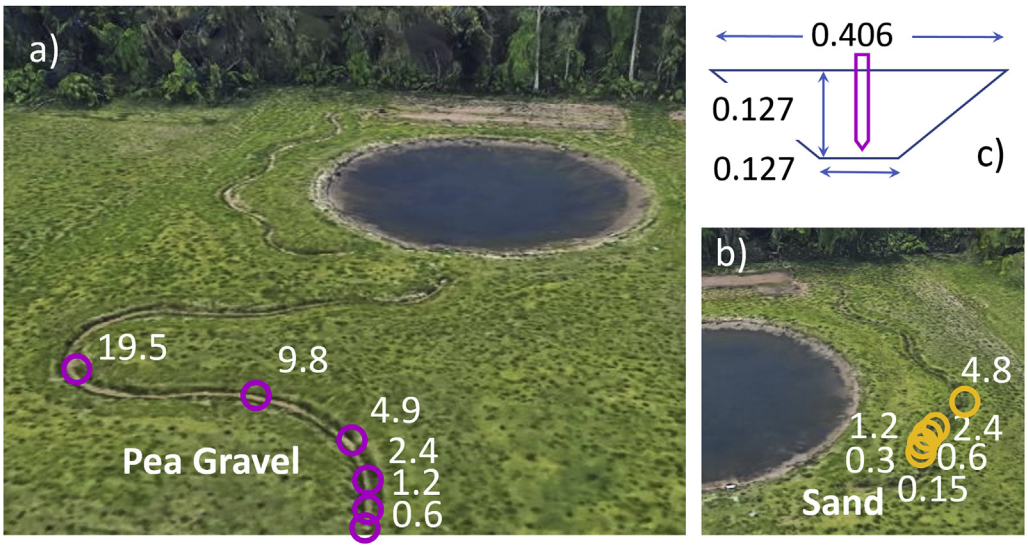

Fig. 1. Aerial images of ND-LEEF site with pea-gravel (a) and sand (b) channels showing sampling locations (distances in meters) in magenta (pea gravel) and yellow (sand) circles. Channel cross section (c) with dimensions shown in meters and sampling centrifuge tube schematic in magenta. (For interpretation of the references to color in this figure legend, the reader is referred to the Web version of this article.)

and approximately 100 ml/min (sand) to saturate each granular media to its surface. Low points on each granular media surface were raised by addition of approximately 1 cm of on-site pea gravel and sand to eliminate overlying water column and channel flow, and thereby restrict flow and transport to underlying granular media (Supplementary Material, Fig. S1). Because the source pool of the sand channel was located downstream from the beginning of that channel, a pit was excavated in the channel immediately upstream to intercept flow upstream that would otherwise enter the channel upstream of the source pool. An unknown fraction of the applied channel source water flowed upstream toward the interception pit.

2.2. Colloid suspensions

Colloids with primary sizes (diameter) ranging from 0.02 to 5.5 μm in pure water were used in the transport experiments: carboxyl-conjugated spherical gold nanoparticles (0.02 μm, 19.32 g/cm^3) (Nanopartz, Loveland CO), yellow-green fluorescent carboxylate-modified polystyrene latex microspheres (CML) (0.2 and 1.0 μm, 1.055 g/cm3, $\lambda_{ex} = 441$ nm, $\lambda_{em} = 486$ nm) (Bangs Laboratories, Inc., Fishers, IN), and non-fluorescent polymethyl methacrylate (PMMA) (5.5 μm, 1.18 g/cm^3) (Bangs Laboratories, Inc., Fishers, IN). Colloid trajectory simulations of gold nanoparticles demonstrated that because of their small size, their interception of surfaces was insensitive to their assumed density in the range from one-half to equality with their single particle density of 19.3 g/cm^3 (Johnson, 2020).

Colloid hydrodynamic radii and electrophoretic mobilities (EPM) were measured using a ζ-potential analyzer (MobiuZ, Wyatt Technology Corp., Santa Barbara, CA). EPM was converted to ζ-potential *via* the Smoluchowski equation for colloid diameters exceeding 100 nm, and *via* the Hückel approximation for colloid diameters <100 nm, for which the colloid diameter was smaller than the Debye length (Ohshima, 1995). Measured colloid hydrodynamic diameters in channel source water were generally higher than those reported by manufacturers, with average diameters of 0.06 ± 0.01, 0.21 ± 0.02 and 1.64 ± 0.14, and 7.75 ± 1.12 μm corresponding to 0.02, 0.2 and 1.0, and 5.5 μm colloids, respectively (Table S1). Whereas modest aggregation was promoted in the elevated IS of site groundwater, aggregate hydrodynamic radii determined via DLS (Supplementary Material, Fig. S4) were stable within 1 h of equilibration with site groundwater (performed at 1:10 dilution) and continuing for the duration of the experiment (i.e., well beyond the 48 h period preceding the low IS pulse). All colloids had negative ζ potentials in site groundwater: −11.76 ± 3.32, −18.1 ± 1.62, −23.44 ± 3.08, and −4.64 ± 1.01 mV for the 0.06, 0.21, 1.6 and 7.7 μm colloids, respectively (Table S2). Colloid ζ-potentials and in site groundwater remained stable far beyond the duration of the experiment (i.e., beyond twelve days; Supplementary Material, Fig. S4).

2.3. Colloid, low IS pulse, and tracer introduction

Source pools (1.5 L, 15 cm width x 8 cm length x 13 cm depth) were located at the zero point of each channel with outflow at the bottom of the downstream face (Supplementary Material). Colloidal suspensions (diluted 1:4 in site groundwater at least 1 h prior to experiment) were introduced at durations (270 and 150 min for pea gravel and sand, respectively) sufficient to produce steady state breakthrough plateaus at all sampled distances from source (Supplementary Material). Measured pool concentrations indicate an additional dilution of approximately 1:200 in site groundwater upon addition of colloid solution to the pool. Following breakthrough and extended elution, a low ionic strength pulse (distilled water) was introduced (270 min) to examine potential colloid reentrainment (Supplementary Material). Prior to introduction of colloid suspension, breakthrough of rhodamine WT dye (Cole-Parmer, Inc.) was examined at selected distances in the pea-gravel to plan sampling frequency and duration.

2.4. Sample collection

Aqueous channel samples downstream from the pool were collected from pre-inserted 15 ml conical centrifuge tubes perforated with approximately 20 2-mm holes. The sampling tubes were inserted vertically into the entire depth of the granular media (Supplementary Material, Fig. S5), and were located at six geometrically spaced distances from the pool (i.e., 0.15, 0.3, 0.61, 1.2, 2.4, and 4.9 m for sand and 0.6, 1.2, 2.4, 4.9, 9.8, and 19.5 m for pea-gravel) (Fig. 1). Samples (10 ml) were collected (approximately 1 and 6 min draw times in pea gravel and sand, respectively) using a

polyethylene tube (30 mm OD) inserted into the perforated conical tubes and connected to a 50 ml syringe. Collected samples were injected into 15 ml conical centrifuge tubes containing 100 μL sodium azide (0.2 M) for preservation, and were refrigerated until analysis. The sampling frequency created sufficient personnel demand between the two channels that sampling in the pea gravel channel was prioritized, since transport experiments for a similar colloid size range in environmental sand media were recently reported (Rasmuson et al., 2019b). Sand sampling frequency was designed to capture breakthrough at longer distances (later times) in the event that field conditions allowed such transport.

After the second elution period following the low IS pulse introduction (second 48-h), granular media samples (200 ml) were excavated across the entire depth at the channel center at each sampling location. Granular media samples were immediately shaken vigorously with 200 ml of distilled water for 1 min to drive detachment of retained microspheres. Syringes were used to collect 10 ml of supernatant, which was stored in 15 ml conical centrifuge tubes, preserved as described for aqueous samples.

2.5. Sample analysis

Colloid concentrations were determined using inductively coupled plasma mass spectrometry (0.06 μm colloids) and flow cytometry calibrated to direct microscopic enumeration. Quantitation limits for relative concentration (C/C_0) (C_0 being the source pool concentration) were 1.2×10^{-3}, 6.8×10^{-5}, 3.7×10^{-4}, and 5.1×10^{-3} for the 0.06, 0.21, 1.6, and 7.7 μm colloids, respectively (Supplementary Material). Details of colloid recovery (mass balance) calculation, determination of experimentally-observed attachment rate coefficients, estimation of theoretically-predicted attachment rate coefficients, and simulated distributions from source are described in Supplementary Material. Due to expense of analysis and the availability of nanoparticle transport information in sand-sized granular media, gold nanoparticle concentrations were not analyzed in the sand channel.

3. Results

3.1. Tracer and colloid breakthrough

Average pore-water velocity in the pea-gravel channel as determined from observed rhodamine breakthrough was 79 ± 1.3 m/day, averaged among the 0.15 and 4.8 m observation distances (Supplementary Material, Fig. S8), which is approximately an order of magnitude higher than nominal velocities reported for sand (several m/day) as expected from the relatively high permeability of gravel. Initial colloid breakthrough in the pea gravel channel was synchronous among all colloid sizes, and also with rhodamine breakthrough at the sampled locations (Fig. 2, Supplementary Material, Fig. S9). Extrapolating rhodamine breakthrough at observed locations to non-sampled distances, according to the solution to the advection-dispersion equation, captured well the timing of colloid breakthrough in the pea gravel (Fig. 2, panel a, Supplementary Material, Fig. S9, dotted black lines), demonstrating that pore water velocity remained constant with distance in the pea gravel channel.

Average steady-state relative breakthrough (C/C_o) of colloids decreased with distance in both the pea gravel and the sand channels, falling below the quantitation limit at distances of 19.5 m in the pea gravel and beyond 0.15 m (and before 0.3 m) in the sand (Fig. 2, panel b, Supplementary Material, Figs. S9 and S10). Initial colloid breakthrough occurred prior to the first sampling time in the sand channel, although elution was well delineated prior to decrease of relative concentrations the below quantitation limit (Supplementary Material, Fig. S9), verifying that transport distances in the streambed-equilibrated sand were consistent with those previously reported in chemically-cleaned sand (Li et al., 2004; Li and Johnson, 2005; Tong et al., 2006) as well as natural sand (Rasmuson et al., 2019b; Johnson, 2020). In both granular media, breakthrough relative concentration was highest for 1.6 μm colloids at all sampling distances where breakthrough was observed (Supplementary Material, Figs. S9 and S10).

Colloid concentrations remained above the quantitation limit (extended tailing) well beyond cessation of injection (extended tailing) at all sampling locations where breakthrough occurred (Fig. 2, Supplementary Material, Figs. S9 and S10). This extended tailing represented colloid dispersion and/or reentrainment (as opposed to slow reduction in source pool concentration), since source pool concentrations dropped below the quantitation limit within 1.5 h (pea gravel) and 12 min (sand) following cessation of injection (Supplementary Material, Fig. S7).

3.2. Trends in attachment rate coefficients (k_f)

Effective attachment rate coefficients (k_f) calculated from average steady-state breakthrough (C/C_o) decreased with increasing transport distance for all colloid sizes across the first 5 m of transport (Fig. 3), with decreases of a factor of three to five among the different colloid sizes. Values of k_f appeared to converge at the 9.8 m distance (Fig. 3), and error bars spanned the range of data at this distance. Beyond this distance, C/C_0 values approached the quantitation limit, such that low confidence was associated with k_f values at the 19.5 m distance.

Decreased effective k_f with distance was not due to overprinting of colloid surfaces by organic matter in groundwater (and potentially decreased attachment) during transport, as demonstrated by relatively constant measured colloid ζ-potentials in site groundwater, which were stable over time periods less than initial breakthrough and longer than the overall potential increase (~33%) (less negative) for 1.6 μm colloids. However, the timescale of this slow increase to modestly less negative values is far greater than the time required for breakthrough within 5 m of the source (<2 h) (Supplementary Material, Fig. S20), and increased ζ-potential during transport would be expected to increase rather than decrease k_f. In the sand channel, colloid breakthrough exceeded the quantitation limit only at the 0.15 m distance (closest to source), verifying that transport distances in the streambed-equilibrated sand (Supplementary Material, Fig. S10) were consistent with those previously reported in chemically-cleaned sand.

Effective attachment rate coefficients were lowest for the 1.6 μm colloid size (Fig. 3, Supplementary Material, Fig. S11). This trend with colloid size occurred in both the pea gravel and sand channels (Fig. 4, Supplementary Material, Fig. S11) at all distances where breakthrough was greater than the quantitation limit, except at the 9.8 m distance in pea gravel where k_f error bars (standard deviations) for all colloid sizes spanned the overall range among the different colloid sizes (Supplementary Material, Fig. S12).

3.3. Colloid reentrainment in response to low ionic strength pulse

In response to the low IS pulse in the pea gravel, aqueous colloid concentrations increased by approximately a factor of five at locations closest to the injection site (i.e., ≤4.9 m) (Fig. 5, Supplementary Material, Fig. S13, panels a–c). Lesser reentrainment response at greater sampling distances presumably reflect reduced IS contrast due to dispersion (Supplementary Material, Fig. S13, panels d–f). In addition to mobilizing colloids, the low IS pulse visibly mobilized organic matter (e.g., algal material, which was also detected in spectroscopic analyses *via* increased background scatter in the *ca.* 7 μm size-range (Supplementary Material, Fig. S14).

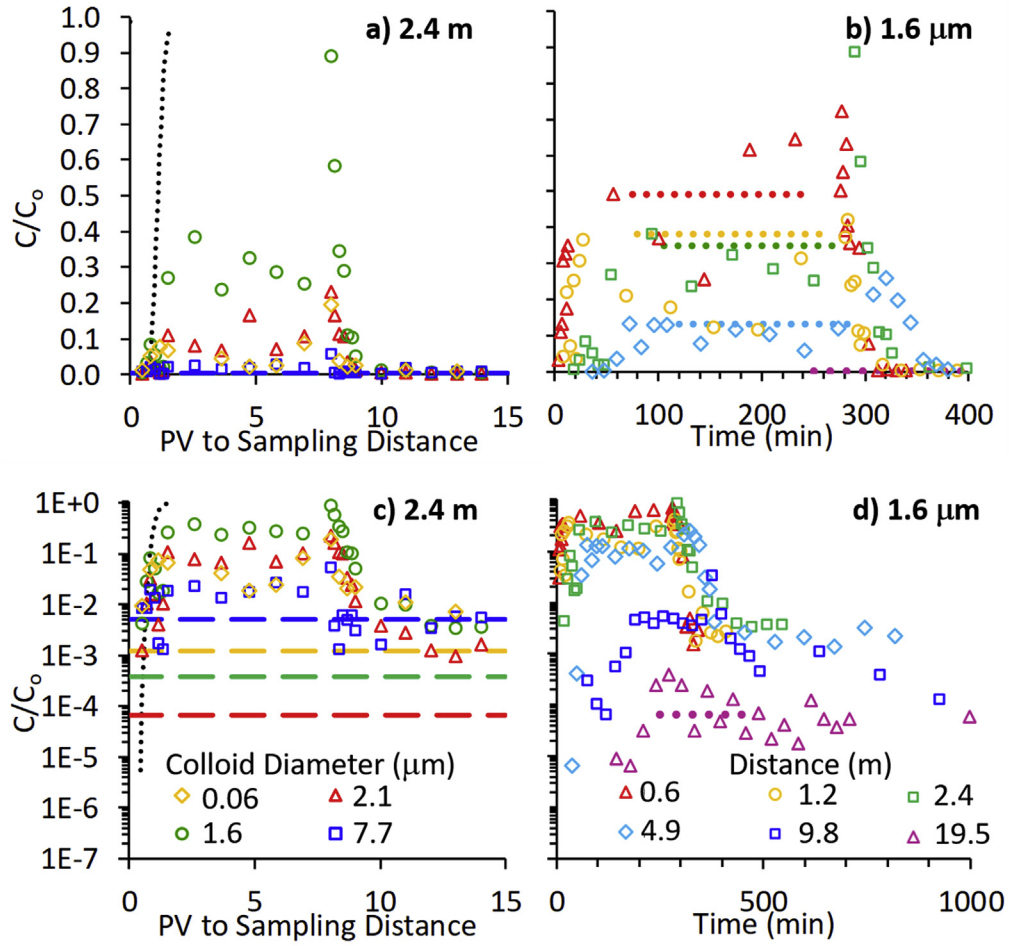

Fig. 2. Panels a (linear) and c (log) show breakthrough-elution concentration histories of all colloid sizes in pea gravel channel at the 2.4 m sampling distance as a function of pore volumes (PV) from source. PV is elapsed time normalized by the calculated average breakthrough time of water for that sampling distance. Panel c shows quantitation limits using horizontal dashed lines in colors corresponding to the legend. Tracer breakthrough predicted by the Ogata-Banks solution (Ogata and Banks, 1961) is shown with the dotted black line in panel c. Panels b (linear) and d (log) show breakthrough-elution concentration histories shown for 1.6 μm colloids as a function of time for multiple sampling distances with average C/Co values shown as dotted lines in colors corresponding to legend in panel d. Breakthrough-elution concentration histories for all colloids at all transport distances are provided in Supplementary Material, Figs. SI-9 and SI-20.

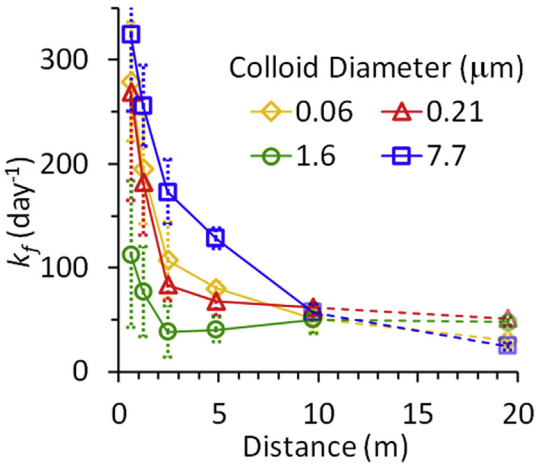

Fig. 3. Attachment rate coefficient (k_f) as a function of distance in the pea gravel channel. Dashed lines and transparent symbols corresponding to 19.5 m distance indicate that breakthrough was below the quantitation limit. Error bars represent the standard deviation of k_f as calculated via error propagation (described in Supplementary Material).

3.4. Sediment profiles

The number concentration of colloids recovered from gravel showed a non-monotonic trend; i.e. a maximum concentration at some distance from the source (Supplementary Material, Fig. S15, symbols). That the distribution of retained colloids was non-monotonic contrasts with the monotonic decrease in k_f with increased transport distance (Fig. 4). This contrast likely reflects mobilization of near-source colloids by the low IS pulse (Fig. 5 and Supplementary Material, Fig. S13), which occurred proximal to the source. The hypothetical distribution of colloids expected from exponential distribution from source was determined using k_f values corresponding to the upstream-most (0.6 m) and downstream-most (9.8 m) locations where k_f was quantifiable (Supplementary Material, Fig. S15, dashed and dotted lines). Superimposing the exponential distributions of retained colloids approximates an expected hyper-exponential distribution, which contrasts against the observed non-monotonic distribution (Supplementary Material, Fig. S15). This contrast is greatest at the upstream-most sampling location, consistent with the observed mobilization of colloids predominantly at locations proximal to source (Fig. 5 and Supplementary Material, Fig. S13).

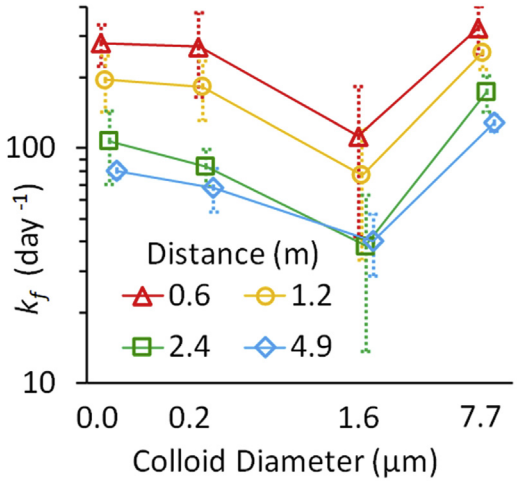

Fig. 4. Attachment rate coefficient (k_f) as a function of colloid diameter (log scale) for pea gravel channel with 0.6, 1.2, 2.4, and 4.9 m sampling locations shown with red triangles, yellow circles, green squares, and blue diamonds, respectively. Note that sizes are staggered slightly around true values to clarify error bars. For distances at which k_f error bars spanned the range of k_f with colloid size (9.8 m distance) or C/C_0 approached quantitation limit (19.5 m distance) (Supplementary Material, Figure SI-12), evaluation of trend of k_f with colloid size was not possible. Error bars represent the standard deviation of k_f as calculated via error propagation (described in Supplementary Material). (For interpretation of the references to color in this figure legend, the reader is referred to the Web version of this article.)

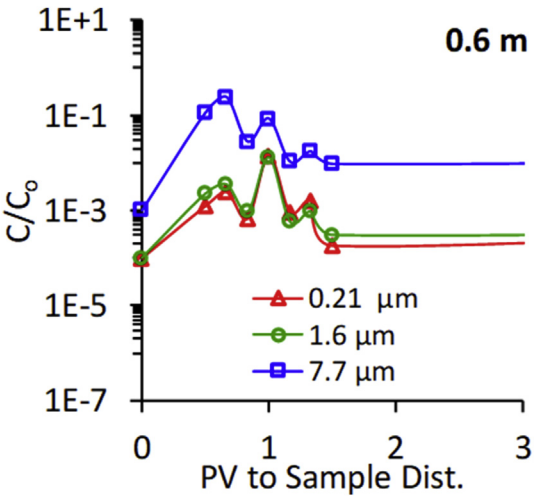

Fig. 5. Colloid concentrations during the low IS pulse for the pea gravel channel at the 0.6 m sampling distance. PV is elapsed time normalized by the calculated average breakthrough time of water for that sampling distance. Colloid concentrations during the low IS pulse at the other sampling locations are provided in the Supplementary Material (Figure SI-13).

4. Discussion

4.1. Non-exponential colloid distribution from source

The observed trend in k_f with transport distance (Fig. 3) for nano-to micro-sized colloids in streambed-equilibrated granular media highlights a major challenge for predicting colloid transport distances in the environment for resource protection or remediation. The approximate factor-of-four k_f reduction (from 240/day to 60/day) across 5 m distance for 0.21 μm colloids (Fig. 3) reduced the colloid removal achieved across that transport distance from 5.3-log (at 0.5 m) to 1.3-log (at 5.0 m). Based on the k_f determined from observed breakthrough at the 0.3 m distance, the relative breakthrough (C/C_0) at 5 m distance would be predicted as 5.1×10^{-6}, which is 4-log greater removal than the observed $C/C_0 = 0.05$ at this distance, a major over-prediction over a modest field transport distance.

Observed colloid transport distances in streambed-equilibrated sand were on the order of centimeters (Supplementary Material, Fig. S10), consistent with those observed under laboratory conditions (e.g., Li et al., 2004; Tufenkji and Elimelech, 2004; Tong et al., 2006; Wang et al., 2014). In contrast, observed colloid transport distances in streambed-equilibrated pea gravel were on the order of meters (Fig. 3). Lesser removal with increasing grain size is an expectation of colloid filtration theory (CFT) (Yao et al., 1971; Rajagopalan and Tien, 1976), since the likelihood that colloids will intercept grains (as quantified by η and k_f) decreases as grain fluid shell thickness increases with increasing grain size. However, the results also demonstrate that in addition to removal, the distance over which non-exponential distribution (effective k_f decrease) occurred also increased with grain size. Hyper-exponential colloid distributions from source extended over similar distances regardless of colloid size ranging over two orders of magnitude (0.06 μm–7.7 μm) (Fig. 3). Given that non-exponential colloid distributions are reported to occur over cm-scale distances in sand-sized granular media (e.g., Li et al., 2004; Tufenkji and Elimelech, 2004; Tong et al., 2006; Wang et al., 2014), the meter-scale hyper-exponential colloid distributions observed in pea gravel demonstrate that non-exponential distributions extend over larger distances in coarser media; i.e., scales with grain size.

The mechanism driving non-exponential colloid distributions from source under unfavorable conditions is a subject of active research (e.g., Hilpert and Johnson, 2018; Johnson et al., 2018; Bedrikovetsky et al., 2019), but the ubiquity of this observation suggests that the mechanism arises from fundamental transport processes. The potential impact on colloid stability of equilibration with aqueous components during transport deserves consideration in field transport studies. Because dilution with site groundwater by approximately 1:4 occurred during colloid suspension preparation, and another approximately 1:200 dilution occurred during introduction to the pool, the potential additional dilution of stock stabilizing surfactants during transport down-gradient from the pool is presumably inconsequential. If colloid aggregation had occurred during transport, one would expect k_f to have increased with increasing transport for the larger (1.6 μm and 7.7 μm) colloids, which is not what was observed. The scaling with grain size demonstrated here is consistent with the hypothesis that the effective k_f decrease is driven by loss of a fast-attaching fraction that is depleted as that fraction of the colloid population attaches to grain surfaces (Johnson et al., 2018). This finding is explored in a separate manuscript (Johnson, 2020) *via* simulations adopting the above hypothesis for description of observations from the streambed-equilibrated pea gravel described here, and from a Wisconsin fine sand (Rasumuson et al., 2019b).

The observed limited colloid transport in the fine sand in this environmental setting suggests that colloid transport behavior over meter-scale and larger distances in fine sand in field settings necessarily involves physical heterogeneity (i.e., preferential transport pathways), for which the relative impacts of colloid-surface interaction is uncharacterized. In contrast, the observed non-exponential colloid distribution in the pea gravel suggests that colloid-surface interaction a dominant control on the observed colloid distributions from source in field settings comprised of coarse granular media such as streambed alluvium.

4.2. Minimum retention for n-μ transition size range

Establishing relevance of laboratory-observed highest colloid mobility in chemically-cleaned media for colloid sizes within the nano-to micro-scale (n-μ) transition size range (i.e., 0.02−2.0 μm) (Ron et al., 2019a) to streambed-equilibrated media (Fig. 4, Supplementary Material, Fig. S11) highlights the opportunity to incorporate this characteristic as a design parameter in colloid-based environmental remediation in granular aquifers. One strategy proposes to aggregate novel nanoparticles to the n-μ transition size range in order to facilitate their transport through non-target porous media, followed by disaggregation at the target location to enhance penetration into granular media pore space and reactivity *via* increased surface area (Ron et al., 2019b).

That colloids of size in the *n-μ* transition and near-neutral buoyancy have highest mobility in granular media has long been known for favorable conditions (Yao et al., 1971; Rajagopalan and Tien, 1976), whereas only recently was it demonstrated that this enhanced mobility is further exaggerated under unfavorable conditions (Ron et al., 2019a). That recognition of this attribute only recently occurred likely reflects that existing field tests have not previously examined, to the knowledge of the authors, a suite of varying colloid sizes while holding surface characteristics relatively constant. However, laboratory column transport of various pathogens (i.e., viruses, bacteria, and protozoa) in Ohio River sand over 3−9 m transport distances reported greatest mobility for bacteria (n-μ transition-sized) relative to the viruses (nano-scale) and protozoa (micro-scale) despite uncontrolled colloid surface properties (Gupta et al., 2009). Field monitoring for pathogens demonstrates greater prevalence of viruses relative to bacteria (Borchardt et al., 2003; Kyle et al., 2008; Eydal et al., 2009; Allen et al., 2017), which nominally contradicts greater mobility of colloids in the n-μ transition size range. However, viruses display lower collision efficiencies (i.e., “stickiness”) than bacteria presumably owing to their surface characteristics (Gannon et al., 1991; Schivjen et al., 2000; Ron et al., 2019a); furthermore, differences in replication/growth and inactivation/death (John and Rose, 2005), ecological predation (Levin, 1977; Lenski, 1988), and source concentrations each may influence relative prevalence of viruses versus bacteria.

The lowest ζ potential was associated with the 1.6 μm colloids, yielding the highest calculated repulsive barrier for that size among the range of colloid sizes examined (Supplementary Material, Fig. S18). However, this lowest ζ potential does not explain the minimum k_f corresponding to this colloid size, since measured properties for all colloid sizes yielded insurmountable repulsive barriers to attachment (>5000 kT) (Supplementary Material, Fig. S18). The barrier was dominated by EDL repulsion for all colloid sizes except 7.7 μm, for which repulsion was dominated by steric interactions. While colloid attachment is qualitatively related to the magnitude of the repulsive barrier (e.g., Torkzaban et al., 2007; Shen et al., 2012), the predicted insurmountability of repulsive barriers requires one of two assumptions regarding attachment; specifically that immobilization occurs either: 1) *via* secondary minimum interactions (e.g., Torkzaban et al., 2007, 2008), or: 2) *via* interaction with nanoscale heterogeneity (e.g., Elimelech and O'Melia, 1990; Duffadar et al., 2007; Pazmino et al., 2014; Rasmuson et al., 2019a; Ron et al., 2019a). Experimental and mechanistic reasons supporting the latter are well reported (Johnson et al., 2010; Pazmino et al., 2014, 2015). A self-consistent outcome of attributing attachment to nanoscale heterogeneity is mechanistic prediction of highest mobility for n-μ transition colloids due to their least likelihood of encountering heterodomains (zones of opposite charge) due to their least combined diffusion, settling, and hydrodynamic drag (Ron et al., 2019a).

4.3. Unfavorable colloid-surface interactions

That non-exponential colloid distributions from source emerge in the laboratory specifically under unfavorable conditions (Li et al., 2004; Tufenkji and Elimelech, 2004a; Tufenkji et al., 2004; Li and Johnson, 2005; Tong and Johnson, 2007; Liang et al., 2013; Wang et al., 2014) suggests that colloid-collector interactions in streambed-equilibrated pea gravel were unfavorable. However, the observed factor of three amplitude (range in k_f across the colloid size range) (Fig. 4) was far less than that observed under highly unfavorable conditions in the laboratory using chemically-cleaned media (Ron et al., 2019a; Rasmuson et al., 2019a), where k_f varied up to three orders of magnitude at the highest pH and lowest IS. The lesser amplitude observed in the pea gravel suggests that conditions in the pea gravel channel (as well as in the sand channel, Supplementary Material, Fig. S11) were not highly unfavorable. That conditions were modestly unfavorable in pea gravel is also supported by the fact that the predicted single-collector k_f from colloid trajectory simulations under favorable conditions bracketed the observed values (Supplementary Material, Fig. S19). The favorable condition simulations were for Happel grain diameters of 446 μm and 6 mm, which are the respective number-based geometric mean and weight-based arithmetic means of pea gravel (Supplementary Material, Fig. S3).

That conditions were unfavorable (albeit modestly) in the pea gravel channel is also supported by the observed colloid detachment in response to solution IS reduction (Fig. 5), which also appears to have altered the observed final colloid distribution in sediment to produce non-monotonic profiles of retained colloids, as described above (Supplementary Material, Fig. S15). Experiments examining colloid release in response to IS perturbation in the laboratory (Ryan and Gschwend, 1994; Roy and Dzombak, 1996; Franchi & O'Melia, 2003; Hahn et al., 2004; Shen et al., 2012; Yi and Chen, 2013) demonstrate that colloid release is negligible when attached colloids were originally loaded under favorable conditions (e.g., Franchi & O'Melia, 2003; Hahn et al., 2004). The reentrainment of colloids in response to a low IS pulse in pea gravel is consistent with unfavorable colloid-surface interaction, suggesting a role of colloid mobilization in reports of increased pathogen prevalence (Curriero et al., 2001; Auld et al., 2004; Dorner et al., 2006) and formation plugging following soil colloid mobilization (McNeal and Coleman, 1966; Frenkel et al., 1978) in response to infiltration of low IS water (i.e., heavy rainfall).

5. Conclusions

The distribution of colloids from source was non-exponential (hyper-exponential) in streambed-equilibrated granular media, demonstrating that equilibration of naturally rough grain surfaces with natural organic matter in the presence of groundwater electrolytes yielded the same complex transport behaviors that emerge under unfavorable conditions in chemically-cleaned granular media under highly controlled conditions. Non-exponential distributions were demonstrated to be consistent for colloids ranging from nano-to micro-sizes and bulk compositions ranging from gold (nano) to polymeric CML and PMMA (micro). Among these colloids with similar surface properties, colloid sizes in the *n-μ* transition size range (0.2−2.0 μm diameter) were most mobile as expected from their least combined diffusion, sedimentation and fluid drag at the grain surface. Non-exponential distribution was described by an effective colloid retention rate coefficient that decreased with increasing distance of transport, which has been mechanistically predicted in chemically-cleaned granular media only under the assumption that a fast-attaching faction of the colloid population is depleted by loss to grain surfaces. The scale over which non-

exponential distribution occurred was consistently greater in coarser media (pea gravel versus fine sand) regardless of colloid size, implicating colloid loss to grain surfaces as a driver of non-exponential distribution. The findings guide development of robust methods to predict non-exponential colloid distribution from source in granular media.

Declaration of competing interest

The authors declare that they have no known competing financial interests or personal relationships that could have appeared to influence the work reported in this paper.

Acknowledgements

This work was developed with support provided by the National Science Foundation under grant numbers DMREF-1629078, CBET-1705770, as well as support from the STAR Fellowship Assistance Agreement no. FP-91780501-0 awarded by the U.S. Environmental Protection Agency. Any opinions, findings, and conclusions or recommendations expressed in this material are those of the authors and do not necessarily reflect the views of the National Science Foundation. This material has not been formally reviewed by EPA. The views expressed in this publication are solely those of the authors, and EPA does not endorse any products or commercial services mentioned in this article.

Appendix A. Supplementary data

Supplementary data to this article can be found online at https://doi.org/10.1016/j.watres.2020.116012.

References

Akaighe, N., Depner, S.W., Banerjee, S., Sharma, V.K., Sohn, M., 2012. The effects of monovalent and divalent cations on the stability of silver nanoparticles formed from direct reduction of silver ions by Suwannee River humic acid/natural organic matter. Sci. Total Environ. 441, 277–289.

Albinger, O., Biesemeyer, B.K., Arnold, R.G., Logan, B.E., 1994. Effect of bacterial heterogeneity on adhesion to uniform collectors by monoclonal populations. FEMS Microbiol. Lett. 124 (3), 321–326.

Allen, A.S., Borchardt, M.A., Kieke, B.A., Dunfield, K.E., Parker, B.L., 2017. Virus occurrence in private and public wells in a fractured dolostone aquifer in Canada. Hydrogeol. J. 25 (4), 1117–1136.

Anderson, A.G., Grose, J., Pahl, S., Thompson, R.C., Wyles, K.J., 2016. Microplastics in personal care products: exploring perceptions of environmentalists, beauticians and students. Mar. Pollut. Bull. 113, 454–460.

Auld, H., MacIver, D., Klaassen, J., 2004. Heavy rainfall and waterborne disease outbreaks: the WALKERTON example. J. Toxicol. Environ. Health Part A 67 (20–22), 1879–1887.

Baalousha, M., Nur, Y., Römer, I., Tejamaya, M., Lead, J.R., 2013. Effect of monovalent and divalent cations, anions and fulvic acid on aggregation of citrate-coated silver nanoparticles. Sci. Total Environ. 454–455, 119–131.

Bedrikovetsky, P., Osipov, Y., Kuzmina, L., Malgaresi, G., 2019. Exact upscaling for transport of size-distributed colloids. Water Resour. Res. 55 (2), 1011–1039.

Bendersky, M., Davis, J.M., 2011. DLVO interaction of colloidal particles with topographically and chemically heterogeneous surfaces. J. Colloid Interface Sci. 353 (1), 87–97.

Bhattacharjee, S., Ko, C.-H., Elimelech, M., 1998. DLVO interaction between rough surfaces. Langmuir 14 (12), 3365–3375.

Bolster, C.H., Mills, A.L., Hornberger, G.M., Herman, J.S., 1999. Spatial distribution of deposited bacteria following miscible displacement experiments in intact cores. Water Resour. Res. 35 (6), 1797–1807.

Borchardt, M.A., Bertz, P.D., Spencer, S.K., Battigelli, D.A., 2003. Incidence of enteric viruses in groundwater from household wells in Wisconsin. Appl. Environ. Microbiol. 69 (2), 1172–1180.

Bradford, S.A., Yates, S.R., Bettahar, M., Simunek, J., 2002. Physical factors affecting the transport and fate of colloids in saturated porous media. Water Resour. Res. 38 (12), 63, 1-63–12.

Curriero, F.C., Patz, J.A., Rose, J.B., Lele, S., 2001. The association between extreme precipitation and waterborne disease outbreaks in the United States , 1948 – 1994. Am. J. Publ. Health 91 (8), 1194–1199.

Davis, J.A., 1982. Adsorption of natural dissolved organic matter at the oxide/water interface. Geochem. Cosmochim. Acta 46 (11), 2381–2393.

Dorner, S.M., Anderson, W.B., Slawson, R.M., Kouwen, N., Huck, P.M., 2006. Hydrologic modeling of pathogen fate and transport. Environ. Sci. Technol. 40 (15), 4746–4753.

Duffadar, R., Davis, J.M., 2007. Interaction of micrometer-scale particles with nanotextured surfaces in shear flow. J. Colloid Interface Sci. 308 (1), 20–29.

Elimelech, M., O'Melia, C.R., 1990. Kinetics of deposition of colloidal particles in porous media. Environ. Sci. Technol. 24 (10), 1528–1536.

Eydal, H.S.C., Jägevall, S., Hermansson, M., Pedersen, K., 2009. Bacteriophage lytic to desulfovibrio aespoeensis isolated from deep groundwater. ISME J. 3 (10), 1139–1147.

Foppen, J.W.A., Schijven, J.F., 2006. Evaluation of data from the literature on the transport and survival of Escherichia coli and thermotolerant coliforms in aquifers under saturated conditions. Water Res. 40 (3), 401–426.

Foppen, J.W., Liem, Y., Schijven, J., 2008. Effect of humic acid on the attachment of Escherichia coli in columns of goethite-coated sand. Water Res. 42 (1–2), 211–219.

Franchi, A., O'Melia, C.R., 2003. Effects of natural organic matter and solution chemistry on the deposition and reentrainment of colloids in porous media. Environ. Sci. Technol. 37 (6), 1122–1129.

Frenkel, H., Goertzen, J.O., Rhoades, J.D., 1978. Effects of clay type and content, exchangeable sodium percentage, and electrolyte concentration on clay dispersion and soil hydraulic conductivity. Soil Sci. Soc. Am. J. 42 (1), 32.

Gannon, J.T., Manilal, V.B., Alexander, M., 1991. Relationship between cell surface properties and transport of bacteria through *soil*. Appl. Environ. Microbiol. 57 (1), 190–193.

Gupta, V., Johnson, W.P., Shafieian, P., Ryu, H., Alum, A., Abbaszadegan, M., Hubbs, S.A., Rauch-Williams, T., 2009. Riverbank filtration: comparison of pilot scale transport with theory. Environ. Sci. Technol. 43 (3), 669–676.

Hahn, M.W., Abadzic, D., O'Melia, C.R., 2004. Aquasols: on the role of secondary minima. Environ. Sci. Technol. 38 (22), 5915–5924.

Han, P., Wang, X., Cai, L., Tong, M., Kim, H., 2014. Transport and retention behaviors of titanium dioxide nanoparticles in iron oxide-coated quartz sand: effects of PH, ionic strength, and humic acid. Colloids Surf. A Physicochem. Eng. Asp. 454, 119–127.

Harvey, R.W., Kinner, N.E., Bunn, A., MacDonald, D., Metge, D., 1995. Transport behavior of groundwater Protozoa and Protozoan-sized microspheres in sandy aquifer sediments. Appl. Environ. Microbiol. 61 (1), 209–217.

Hilpert, M., Johnson, W.P., 2018. A binomial modeling approach for upscaling colloid transport under unfavorable attachment conditions: emergent prediction of nonmonotonic retention profiles. Water Resour. Res. 54 (1), 46–60.

Huynh, K.A., Chen, K.L., 2011. Aggregation kinetics of citrate and polyvinylpyrrolidone coated silver nanoparticles in monovalent and divalent electrolyte solutions. Environ. Sci. Technol. 45 (13), 5564–5571.

Israelachvili, J.N., 2011. Intermolecular and Surface Forces, third ed. Academic Press, Burlington, MA, USA.

Jardine, P.M., McCarthy, J.F., Weber, N.L., 1989. Mechanisms of dissolved organic carbon adsorption on soil. Soil Sci. Soc. Am. J. 53 (5), 1378–1385.

Jin, C., Normani, S.D., Emelko, M.B., 2015. Surface roughness impacts on granular media filtration at favorable deposition conditions: experiments and modeling. Environ. Sci. Technol. 49 (13), 7879–7888.

John, D.E., Rose, J.B., 2005. Review of factors affecting microbial survival in groundwater. Environ. Sci. Technol. 39 (19), 7345–7356.

Johnson, P.R., Sun, N., Elimelech, M., 1996. Colloid transport in geochemically heterogeneous porous Media : modeling and measurements colloid transport in geochemically heterogeneous porous Media : modeling and measurements. Environ. Sci. Technol. 30 (11), 3284–3293.

Johnson, P., Zhang, P., Fuller, M.E., Scheibe, T.D., Mailloux, B.J., Onstott, T.C., DeFlaun, M.F., Hubbard, S.S., Radtke, J., Kovacik, W.P., et al., 2001. Ferrographic tracking of bacterial transport in the field at the narrow channel focus area, oyster, VA. Environ. Sci. Technol. 35 (1), 182–191.

Johnson, W.P., Hilpert, M., 2013. Upscaling colloid transport and retention under unfavorable conditions: linking mass transfer to pore and grain topology. Water Resour. Res. 49 (9), 5328–5341.

Johnson, W.P., Logan, B.E., 1996. Enhanced transport of bacteria in porous media by sediment-phase and aqueous-phase natural organic matter. Water Res. 30 (4), 923–931.

Johnson, W.P., Pazmino, E., Ma, H., 2010. Direct observations of colloid retention in granular media in the presence of energy barriers, and implications for inferred mechanisms from indirect observations. Water Res. 44 (4), 1158–1169.

Johnson, W.P., Rasmuson, A., Pazmiño, E., Hilpert, M., 2018. Why variant colloid transport behaviors emerge among identical individuals in porous media when colloid–surface repulsion exists. Environ. Sci. Technol. 52 (13), 7230–7239.

Johnson, W.P., 2020. Quantitative linking of nanoscale interactions to continuum-scale nanoparticle and microplastic transport in environmental granular media. Environ. Sci. Technol. https://doi.org/10.1021/acs.est.0c01172.

Kyle, J.E., Eydal, H.S.C., Ferris, F.G., Pedersen, K., 2008. Viruses in granitic groundwater from 69 to 450 m depth of the Äspö hard Rock laboratory, Sweden. ISME J. 2 (5), 571–574.

Laumann, S., Micić, V., Hofmann, T., 2014. Mobility enhancement of nanoscale zero-valent iron in carbonate porous media through Co-injection of polyelectrolytes. Water Res. 50, 70–79.

Laumann, S., Micić, V., Lowry, G.V., Hofmann, T., 2013. Carbonate minerals in porous media decrease mobility of polyacrylic acid modified zero-valent iron nanoparticles used for groundwater remediation. Environ. Pollut. 179, 53–60.

Lenski, R.E., 1988. Dynamics of interactions between bacteria and virulent

bacteriophage. In: Advances in Microbial Ecology. Plenum Press, New York, NY, USA, pp. 1–44.
Levin, B.R., Stewart, F.M., Chao, L., 1977. Resource-limited growth, competition, and predation: a model and experimental studies with bacteria and bacteriophage. Am. Nat. 111 (977), 3–24.
Li, X., Johnson, W.P., 2005. Nonmonotonic variations in deposition rate coefficients of microspheres in porous media under unfavorable deposition conditions. Environ. Sci. Technol. 39 (6), 1658–1665.
Li, X., Scheibe, T.D., Johnson, W.P., 2004. Apparent decreases in colloid deposition rate coefficients with distance of transport under unfavorable deposition conditions: a general phenomenon. Environ. Sci. Technol. 38 (21), 5616–5625.
Liang, Y., Bradford, S.A., Simunek, J., Vereecken, H., Klumpp, E., 2013. Sensitivity of the transport and retention of stabilized silver nanoparticles to physicochemical factors. Water Res. 47 (7), 2572–2582.
Liu, X., O'Carroll, D.M., Petersen, E.J., Huang, Q., Anderson, C.L., 2009. Mobility of multiwalled carbon nanotubes in porous media. Environ. Sci. Technol. 43 (21), 8153–8158.
Liu, Y., Yang, C., Li, J., 2007. Influence of extracellular polymeric substances on Pseudomonas aeruginosa transport and deposition profiles in porous media. Environ. Sci. Technol. 41 (1), 198–205.
McNeal, B.L., Coleman, N.T., 1966. Effect of solution composition on soil hydraulic Conductivity1. Soil Sci. Soc. Am. J. 30 (3), 308.
Ogata, A., Banks, R., 1961. A solution of the differential equation of longitudinal dispersion in porous media. Geol. Surv. Prof. Pap.
Ohshima, H., 1995. Electrophoretic mobility of soft particles. Colloids Surf., A 103 (3), 249–255.
Panno, S.V., Kelly, W.R., Scott, J., Zheng, W., McNeish, R.E., Holm, N., Hoellein, T.J., Baranski, E.L., 2019. Microplastic Contamination in Karst Groundwater Systems. Groundwater 57 (2), 189–196.
Pazmino, E., Trauscht, J., Dame, B., Johnson, W.P., 2014. Power law size-distributed heterogeneity explains colloid retention on soda lime glass in the presence of energy barriers. Langmuir 30 (19), 5412–5421.
Pelley, A.J., Tufenkji, N., 2008. Effect of particle size and natural organic matter on the migration of nano- and microscale latex particles in saturated porous media. J. Colloid Interface Sci. 321 (1), 74–83.
Rajagopalan, R., Tien, C., 1976. Trajectory analysis of deep-bed filtration with the sphere-in-cell porous media model. AIChE J. 22 (3), 523–533.
Rasmuson, A., Pazmino, E., Assemi, S., Johnson, W.P., 2017. Contribution of nano- to microscale roughness to heterogeneity: closing the gap between unfavorable and favorable colloid attachment conditions. Environ. Sci. Technol. 51 (4), 2151–2160.
Rasmuson, A., VanNess, K., Ron, C.A., Johnson, W.P., 2019a. Hydrodynamic versus surface interaction impacts of roughness in closing the gap between favorable and unfavorable colloid transport conditions. Environ. Sci. Technol. 53 (5), 2450–2459.
Rasmuson, A., Erickson, B., Borchardt, M., Muldoon, M., Johnson, W.P., 2019b. Pathogen prevalence in fractured versus granular aquifers and the role of forward flow stagnation zones on pore scale delivery to surfaces. Environ. Sci. Technol. 54 (1), 137–145.
Ray, C., D'Alessio, M., Sobotková, M., Mohanram, A., Jenkins, M., Sněhota, M., 2019. Comparing transport of cryptosporidium -sized carboxylated microspheres in two undisturbed soil cores under unsaturated conditions. J. Environ. Eng. 145 (4), 06019002.
Ron, C.A., Dong, M., Wooley, K.L., Johnson, W.P., 2019. Theory-guided targeted delivery of nanoparticles in advective environmental porous media. Environ. Sci. Technol. Lett. 6 (10), 617–623.
Ron, C.A., VanNess, K., Rasmuson, A., Johnson, W.P., 2019. How nanoscale surface heterogeneity impacts transport of nano- to micro-particles on surfaces under unfavorable attachment conditions. Environ. Sci. Nano 6 (6), 1921–1931.
Roy, S.B., Dzombak, D.A., 1996. Na+-Ca2+ exchange effects in the detachment of latex colloids deposited in glass bead porous media. Colloids Surf. A Physicochem. Eng. Asp. 119 (2–3), 133–139.
Ryan, J.N., Elimelech, M., Ard, R.A., Harvey, R.W., Johnson, P.R., 1999. Bacteriophage PRD1 and silica colloid transport and recovery in an iron oxide-coated sand aquifer. Environ. Sci. Technol. 33 (1), 63–73.
Ryan, J.N., Gschwend, P.M., 1994. Effects of ionic strength and flow rate on colloid release: relating kinetics to intersurface potential energy. J. Colloid Interface Sci. 164 (1), 21–34.
Scheibe, T.D., Hubbard, S.S., Onstott, T.C., DeFlaun, M.F., 2011. Lessons learned from bacterial transport research at the South oyster site. Ground Water 49 (5), 745–763.
Schijven, J.F., Hoogenboezem, W., Hassanizadeh, S.M., Peters, J.H., 1999. Modeling removal of bacteriophages MS2 and PRD1 by dune recharge at castricum, Netherlands. Water Resour. Res. 35 (4), 1101–1111.
Schijven, J.F., Medema, G., Vogelaar, A.J., Hassanizadeh, S.M., 2000. Removal of microorganisms by deep well injection. J. Contam. Hydrol. 44 (3–4), 301–327.
Scholl, M.A., Harvey, R.W., 1992. Laboratory investigations on the role of sediment surface and groundwater chemistry in transport of bacteria through A contaminated sandy aquifer. Environ. Sci. Technol. 26 (7), 1410–1417.
Schwarzenbach, R.P., Gschwend, P.M., Imboder, D.M., 1993. Environmental Organic Chemistry, second ed. Wiley Interscience, New York, NY, USA.
Shen, C., Wang, L.P., Li, B., Huang, Y., Jin, Y., 2012. Role of surface roughness in chemical detachment of colloids deposited at primary energy minima. Vadose Zone J. 11 (1).
Tipping, E., Cooke, D., 1982. The effects of adsorbed humic substances on the surface charge of goethite (α-FeOOH) in freshwaters. Geochem. Cosmochim. Acta 46 (1), 75–80.
Tong, M., Johnson, W.P., 2007. Colloid population heterogeneity drives hyperexponential deviation from classic filtration theory. Environ. Sci. Technol. 41 (2), 493–499.
Tong, M., Johnson, W.P., 2006. Excess colloid retention in porous media as a function of colloid size, fluid velocity, and grain angularity. Environ. Sci. Technol. 40 (24), 7725–7731.
Tong, M., Li, X., Brow, C.N., Johnson, W.P., 2005. Detachment-influenced transport of an adhesion-deficient bacterial strain within water-reactive porous media. Environ. Sci. Technol. 39 (8), 2500–2508.
Torkzaban, S., Bradford, S.A., Walker, S.L., 2007. Resolving the coupled effects of hydrodynamics and DLVO forces on colloid attachment in porous media. Langmuir 23 (19), 9652–9660.
Torkzaban, S., Tazehkand, S.S., Walker, S.L., Bradford, S.A., 2008. Transport and fate of bacteria in porous media: coupled effects of chemical conditions and pore space geometry. Water Resour. Res. 44 (4), 1–12.
Trauscht, J., Pazmino, E., Johnson, W.P., 2015. Prediction of nanoparticle and colloid attachment on unfavorable mineral surfaces using representative discrete heterogeneity. Langmuir 31 (34), 9366–9378.
Tufenkji, N., Elimelech, M., 2005. Breakdown of colloid filtration theory: role of the secondary energy minimum and surface charge heterogeneities. Langmuir 21 (3), 841–852.
Tufenkji, N., Elimelech, M., 2004. Deviation from the classical colloid filtration theory in the presence of repulsive DLVO interactions. Langmuir 20 (25), 10818–10828.
Tufenkji, N., Elimelech, M., 2005. Spatial distributions of cryptosporidium oocysts in porous media: evidence for dual mode deposition. Environ. Sci. Technol. 39 (10), 3620–3629.
Tufenkji, N., Miller, G.F., Ryan, J.N., Harvey, R.W., Elimelech, M., 2004. Transport of cryptosporidium oocysts in porous media: role of straining and physicochemical filtration. Environ. Sci. Technol. 38 (22), 5932–5938.
Wang, D., Bradford, S.A., Harvey, R.W., Gao, B., Cang, L., Zhou, D., 2012. Humic acid facilitates the transport of ARS-labeled hydroxyapatite nanoparticles in iron oxyhydroxide-coated sand. Environ. Sci. Technol. 46 (5), 2738–2745.
Wang, D., Ge, L., He, J., Zhang, W., Jaisi, D.P., Zhou, D., 2014. Hyperexponential and nonmonotonic retention of polyvinylpyrrolidone-coated silver nanoparticles in an *ultisol*. J. Contam. Hydrol. 164, 35–48.
Worthington, S.R.H., Smart, C.C., 2017. Transient bacterial contamination of the dual-porosity aquifer at walkerton, ontario, Canada. Hydrogeol. J. 25 (4), 1003–1016.
Yao, K., Habibian, M.T., O'Melia, C.R., 1971. Water and waste water filtration: concepts and applications. Environ. Sci. Technol. 5 (11), 1105–1112.
Yi, P., Chen, K.L., 2013. Influence of solution chemistry on the release of multiwalled carbon nanotubes from silica surfaces. Environ. Sci. Technol. 47 (21), 12211–12218.
Zhang, P., Johnson, W.P., Scheibe, T.D., Choi, K., Dobbs, F.C., Mailloux, B.J., 2001. Extended tailing of bacteria following breakthrough at the narrow channel focus area, oyster, Virginia. Water Resour. Res. 37 (11), 2687–2698.
Zhang, W., 2003. Nanoscale iron particles for environmental Remediation : an overview. J. Nanoparticle Res. 5, 323–332.
Zhang, Y., Diehl, A., Lewandowski, A., Gopalakrishnan, K., Baker, T., 2020. Removal efficiency of micro- and nanoplastics (180 nm–125 μm) during drinking water treatment. Sci. Total Environ. 720, 137383.